Springer

KSME

Journal of Mechanical Science and Technology 24 (2) (2010) 505~512
www.springerlink.com/content/1738-494x
DOI 10.1007/s12206-009-1213-7

Effect of a viscous fluid at the end face on the torsional vibration of a rod †

Jin Oh Kim* and Han Yong Chun

Department of Mechanical Engineering, Soongsil University, Seoul, 156-743, Korea

(Manuscript Received May 8, 2009; Revised October 10, 2009; Accepted November 9, 2009)

Abstract

This paper deals with the effect of an adjacent viscous fluid on the torsional vibration of a circular rod. The rod is in contact with the viscous fluid at one end face, and the other end face is torsionally excited by a transducer. The interaction between the torsional vibration of the rod and the fluid has been studied theoretically. Expressions for the natural frequencies and damping rate of the torsional vibration have been obtained through exact and approximate solutions.

Keywords: Torsional vibration; Viscous fluid; Fluid-structure interaction; Natural frequency; Damping rate

1. Introduction

The interaction between the torsional vibration of a circular rod and an adjacent viscous fluid has been applied to the measurement of the fluid viscosity [1]. In the torsional vibration of a circular rod submerged in a viscous fluid, the motion of the solid exerts shear stress to the surrounding viscous fluid. Meanwhile, the fluid resists the motion of the solid, and in so doing the vibrational characteristics of the solid rod are affected. The rod plays the role of a viscosity sensor.

In the previous research [1], the circumferential face of a circular rod was considered to be in contact with a viscous fluid. The cross-sectional area of the rod was much smaller than the circumferential area, and the effect of the viscous fluid on the motion of the end face was negligibly small. If the cross-sectional area of the rod is not much smaller than the circumferential area, the effect of a viscous fluid at the end face on the torsional vibration of a rod should not be neglected.

Depending on the measurement environment, the size of the sensor is restricted. In an oil chamber of a car engine, for example, a sensor should be compact. In fact, many researchers are attempting to monitor the condition of engine oil by measuring the variation of the oil viscosity [2-4]. Torsional vibration viscometer would be one promising apparatus, if the rod is short enough.

This paper deals with an interaction problem between an elastic rod and a viscous fluid. The elastic rod is considered to be short but thick such that the length is same to or less than the thickness; meanwhile, the previous study [1] considered a long but thin rod which is in contact with a viscous fluid at the circumference face. A circular rod, as shown in Fig. 1, is in contact with a viscous fluid at one end face. The other end face is torsionally excited by a transducer. The torsional transducer was reported earlier [5]. To evaluate the natural frequencies and damping rate, the end face is assumed to be fixed on a rigid transducer. The effect of an adjacent viscous fluid on the torsional vibration of a circular rod is theoretically obtained through exact and approximate solutions.

2. Formulation of the fluid-structure interaction

A circular rod, as shown in Fig. 1, is in contact with a viscous fluid at one end face ($z = 0$) and is fixed at the other end ($z = -L$). The rod has shear modulus G and mass density ρ_s, and the fluid has viscosity μ and mass density ρ_f. The length of the rod is L and the radius of the cross-section is r_o. Torsional vibration is formulated in this section.

The equation of motion for the rod, which obeys Hooke's law, is expressed in terms of the circumferential displacement $u_\theta(r,z,t)$ as follows [6]:

$$\rho_s \frac{\partial^2 u_\theta}{\partial t^2} = G\left(\frac{\partial^2 u_\theta}{\partial r^2} + \frac{1}{r}\frac{\partial u_\theta}{\partial r} - \frac{u_\theta}{r^2} + \frac{\partial^2 u_\theta}{\partial z^2} \right) \qquad (1)$$

$$-L \le z \le 0, \quad 0 \le r \le r_0$$

The vibration induced by the torsional motion of the rod is assumed to have linear characteristic. The equation of motion for the Newtonian fluid is expressed in terms of the circumferential velocity $v_\theta(r,z,t)$ as follows [7]:

† This paper was recommended for publication in revised form by Associate Editor Yeon June Kang

*Corresponding author. Tel.: +82 2 820 0662, Fax.: +82 2 820 0668
E-mail address: jokim@ssu.ac.kr

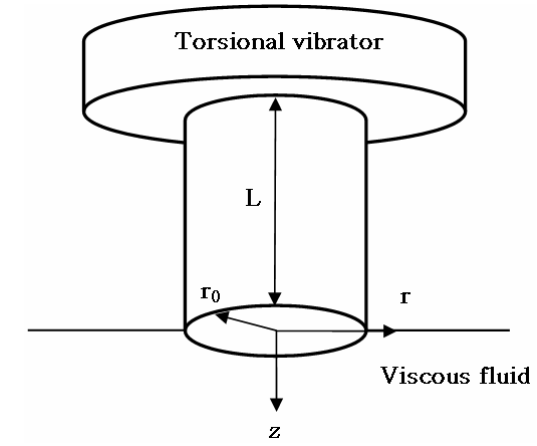

(a)

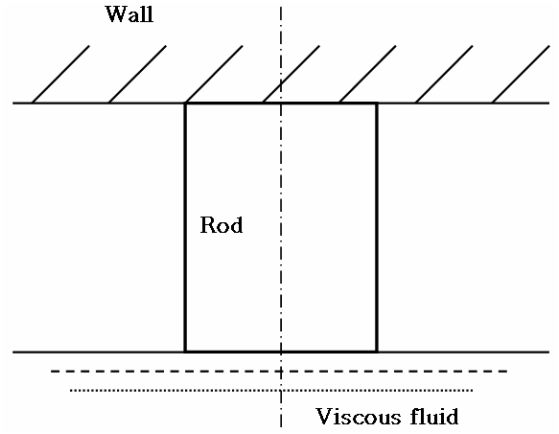

(b)

Fig. 1.Schematic diagram of a circular rod in contact with a viscous fluid at one end face.

$$\rho_f \frac{\partial v_\theta}{\partial t} = \mu\left(\frac{\partial^2 v_\theta}{\partial r^2} + \frac{1}{r}\frac{\partial v_\theta}{\partial r} - \frac{v_\theta}{r^2} + \frac{\partial^2 v_\theta}{\partial z^2}\right) \quad (2)$$

$0 \le z < \infty$

Since one end ($z = -L$) of the rod is fixed and the circumferential face is assumed traction-free, the boundary conditions for the rod are as follows:

$$u_\theta = 0 \text{ at } 0 \le r \le r_0 \text{ and } z = -L \quad (3)$$

$$u_\theta = 0 \text{ at } r = 0 \text{ and } -L \le z \le 0 \quad (4)$$

$$\frac{\partial u_\theta}{\partial r} - \frac{u_\theta}{r} = 0 \text{ at } r = r_0 \text{ and } -L \le z \le 0 \quad (5)$$

The boundary conditions for the fluid are as follows:

$$\frac{\partial v_\theta}{\partial r} = 0 \text{ at } r_0 < r < \infty \text{ and } z = 0 \quad (6)$$

$$v_\theta \to 0 \text{ at } 0 \le r < \infty \text{ and } z \to \infty \quad (7a)$$

$$v_\theta \to 0 \text{ at } r \to \infty \quad (7b)$$

The continuities of the shear stress and vibration velocity at the interface of the solid rod and viscous fluid provide the following interface conditions:

$$\frac{\partial u_\theta}{\partial t} = v_\theta \text{ at } 0 \le r \le r_0 \text{ and } z = 0 \quad (8)$$

$$G\frac{\partial u_\theta}{\partial z} = \mu\frac{\partial v_\theta}{\partial z} \text{ at } 0 \le r \le r_0 \text{ and } z = 0 \quad (9)$$

All quantities in Eqs. (1)-(9) are nondimensionalized by using the length scale r_0, velocity scale $c_0\,[=(G/\rho_s)^{1/2}]$, and time scale r_0/c_0. The equations are expressed in terms of the nondimensional displacement u of the solid rod, nondimensional velocity v of the fluid, and the nondimensional variables $\xi\ (=r/r_0)$, $\varsigma\ (=z/r_0)$, and $\tau\ (=t\ c_0/r_0)$ as follows:

$$\frac{\partial^2 u}{\partial \tau^2} = \frac{\partial^2 u}{\partial \xi^2} + \frac{1}{\xi}\frac{\partial u}{\partial \xi} - \frac{u}{\xi^2} + \frac{\partial^2 u}{\partial \varsigma^2} \quad (10)$$

$-l \le \varsigma \le 0,\ 0 \le \xi \le 1$

$$\frac{\partial v}{\partial \tau} = \frac{1}{R}\left(\frac{\partial^2 v}{\partial \xi^2} + \frac{1}{\xi}\frac{\partial v}{\partial \xi} - \frac{v}{\xi^2} + \frac{\partial^2 v}{\partial \varsigma^2}\right) \quad (11)$$

$0 \le \varsigma < \infty$

$$u = 0 \text{ at } 0 \le \xi \le 1 \text{ and } \varsigma = -l \quad (12)$$

$$u = 0 \text{ at } \xi = 0 \text{ and } -l \le \varsigma \le 0 \quad (13)$$

$$\frac{\partial u}{\partial \xi} - \frac{u}{\xi} = 0 \text{ at } \xi = 1 \text{ and } -l \le \varsigma \le 0 \quad (14)$$

$$\frac{\partial v}{\partial \varsigma} = 0 \text{ at } 1 < \xi < \infty \text{ and } \varsigma = 0 \quad (15)$$

$$v \to 0 \text{ at } 0 \le \xi < \infty \text{ and } \varsigma \to \infty \quad (16a)$$

$$v \to 0 \text{ at } \xi \to \infty \quad (16b)$$

$$\frac{\partial u}{\partial \tau} = v \text{ at } 0 \le \xi \le 1 \text{ and } \varsigma = 0 \quad (17)$$

$$\frac{\partial u}{\partial \varsigma} = \frac{\rho}{R}\frac{\partial v}{\partial \varsigma} \text{ at } 0 \le \xi \le 1 \text{ and } \varsigma = 0 \quad (18)$$

Here $\rho = \rho_f/\rho_s$, $R = \rho_f\, r_0\, c_0/\mu$, and $l = L/r_0$. R is inversely proportional to the viscosity, similar to the definition of Reynolds number.

3. Exact solutions

3.1 General modes

The solution of Eq. (10) has the following form:

$$u(\xi,\varsigma,\tau) = X(\xi)\ U(\varsigma)\ \exp[i(\omega + ih)\tau] \quad (19)$$

The solution of Eq. (11) is divided into the interior solution v_i for the interior region ($0 \le \xi \le 1$) and the outer solution v_o for the outer region ($1 \le \xi \le \infty$), and they have the following forms:

$$v_i(\xi,\varsigma,\tau) = X(\xi)\ V(\varsigma)\ \exp[i(\omega + ih)\tau] \quad (20a)$$

$$v_o(\xi,\varsigma,\tau) = Y(\xi)\ V(\varsigma)\ \exp[i(\omega + ih)\tau] \quad (20b)$$

where ω (= $\tilde{\omega}\, r_0/c_0$) and h (= $\tilde{h}\, r_0/c_0$) are the nondimensional forms of the natural frequency $\tilde{\omega}$ and damping rate per unit time $\tilde{h}$.

Substituting Eq. (19) into Eq. (10) yields the following:

$$U'' + k_1^2 U = 0 \tag{21a}$$

$$\xi^2 X'' + \xi X' - (p^2 \xi^2 + 1) X = 0 \tag{21b}$$

where $p^2 = k_1^2 - (\omega + ih)^2$. The solutions of Eqs. (21a) and (21b) have the following forms:

$$U(\varsigma) = c_1 \sin k_1\varsigma + c_2 \cos k_1\varsigma \tag{22a}$$

$$X(\xi) = d_1 I_1(p\xi) + d_2 K_1(p\xi) \tag{22b}$$

Substituting Eq. (19) into the boundary conditions (12)~(14) yields the following:

$$U(-l) = 0 \tag{23a}$$

$$X(0) = 0 \tag{23b}$$

$$X'(1) - X(1) = 0 \tag{23c}$$

Substituting Eqs. (22a)- (22b) into Eqs. (23a)- (23c) results in the following equations:

$$-c_1 \sin k_1 l + c_2 \cos k_1 l = 0 \tag{24a}$$

$$d_2 = 0 \tag{24b}$$

$$I_1'(p) - I_1(p) = p\, I_2(p) = 0 \tag{24c}$$

Eq. (22a), after Eq. (24a) has been applied to, becomes as follows:

$$U(\varsigma) = c_1 \sin k_1(\varsigma + l) \tag{25a}$$

Eq. (22b) with Eq. (24b) and Eq. (25a) are substituted in Eq. (19), then Eq. (19) becomes:

$$u(\xi,\varsigma,\tau) = A \sin k_1(\varsigma + l)\, I_1(p\xi) \exp[i(\omega + ih)\tau] \tag{25b}$$

Substituting Eq. (20a) into Eq. (11) yields the following:

$$V'' - k_2^2 V = 0 \tag{26}$$

where $k_2^2 = -p^2 + i(\omega + ih)R$. The boundary condition (16a) reduces to

$$V(\infty) = 0 \tag{27}$$

The solution of Eq. (26) satisfying the boundary condition (27) has the following form:

$$V(\varsigma) = c_3 \exp(-k_2 \varsigma) \tag{28}$$

Among the modes corresponding to the roots p of Eq. (24c), the fundamental mode is the main interest.

3.2 Fundamental mode

The lowest value of the roots p is 0, and the fundamental mode along the radial coordinate has the following relationship:

$$k_1^2 - (\omega + ih)^2 = 0 \tag{29}$$

In this case, Eq. (21b) for the solid region becomes

$$\xi^2 X'' + \xi X' - X = 0 \tag{30}$$

With the boundary condition (23b), the solution of Eq. (30) is as follows:

$$X(\xi) = a\, \xi \tag{31}$$

Substituting Eq. (31) and (25a) into Eq. (19) yields the following:

$$u(\xi,\varsigma,\tau) = A\, \xi \sin k_1(\varsigma + l) \exp(i\, k_1\, \tau) \tag{32}$$

Meanwhile, substituting Eq. (20b) into Eq. (11) yields the following equation for the fundamental mode:

$$\xi^2 Y'' + \xi Y' - Y = 0 \tag{33}$$

Since the boundary condition (16b) reduces to $Y(\infty) = 0$, the solution of Eq. (33) becomes

$$Y(\xi) = b\, \frac{1}{\xi} \tag{34}$$

Substituting Eqs. (31) and (28) into Eq. (20a) yields the following:

$$v_i(\xi,\varsigma,\tau) = B\, \xi \exp(-\sqrt{i\, k_1 R}\ \varsigma) \exp(i\, k_1\, \tau) \tag{35}$$

Similarly, substituting Eqs. (34) and (28) into Eq. (20b) yields the following:

$$v_o(\xi,\varsigma,\tau) = C\, \frac{1}{\xi} \exp(-\sqrt{i\, k_1 R}\ \varsigma) \exp(i\, k_1\, \tau) \tag{36}$$

Continuity at $\xi = 1$ is expressed by $v_i(1) = v_o(1)$, and hence the following relation is obtained:

$$B = C \tag{37}$$

The solutions u and v expressed by Eqs. (32) and (35), respectively, satisfy the interface condition (17)-(18).

$$i\, k_1 A \sin k_1 l = B \tag{38}$$

$$A\, k_1 \cos k_1 l = \frac{\rho}{R} (-\sqrt{i\, k_1 R})\, B \tag{39}$$

In order for Eqs. (37)- (39) to have nontrivial solutions for A, B, C, the following characteristic equation is obtained:

$$\frac{\rho}{R} \sqrt{i\, k_1 R} \cdot i\, k_1 \sin k_1 l + k_1 \cos k_1 l = 0 \tag{40}$$

Eq. (40) can be rewritten as

$$\tan k_1 l = \frac{\sqrt{i}\,\sqrt{R\,l}}{\rho} \cdot \frac{1}{\sqrt{k_1\,l}} \tag{41}$$

Eq. (41) is a complex equation that provides implicit relationships between (ω, h) and (R, ρ), i.e., $\omega = \omega(R, \rho)$ and $h = h(R, \rho)$. The solution of Eq. (41) can be easily obtained by using a root-finding function available, for example, in Mathematica [8].

For the fundamental mode both in the radial coordinate and in the axial coordinate, the natural frequency ω and the damping rate h were calculated for the case of $l = 2$. In Fig. 2, the calculated results are displayed by symbols as functions of the fluid viscosity (R) for three density ratios ρ = 0.1, 0.5, 1.0. The solid lines in Fig. 2 correspond to asymptotic solutions which will be described in the next section. In Fig. 2 (a), $\omega_0 = \pi/(2l)$, which is the natural frequency without the effect of the viscous fluid, i.e., $R \to \infty$.

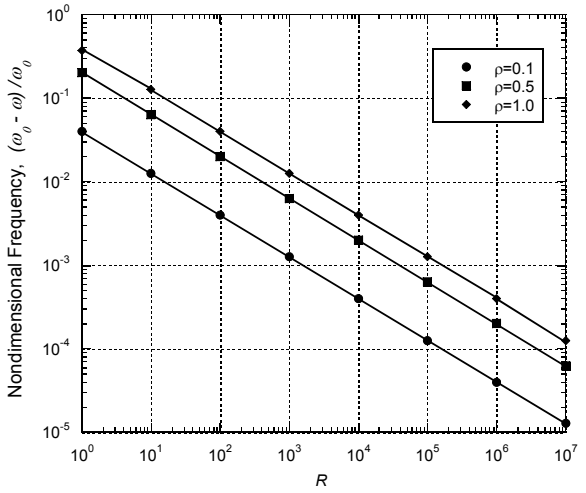

(a)

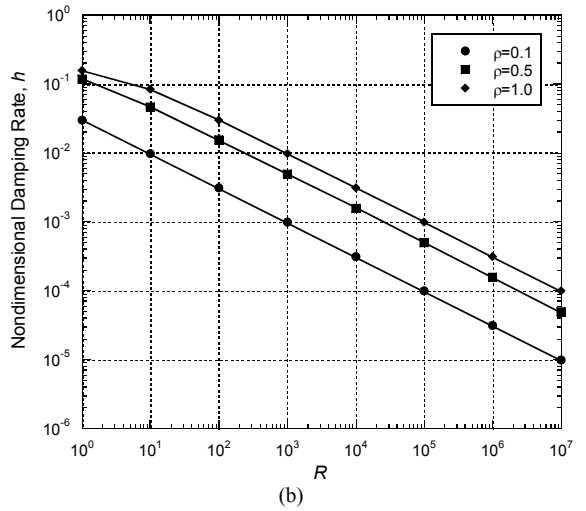

(b)

Fig. 2. Exact solutions (symbols) and approximate solutions (lines) depicted as a function of R for ω = 1.0 and various ρ. (a) nondimensional frequency, (b) nondimensional damping rate.

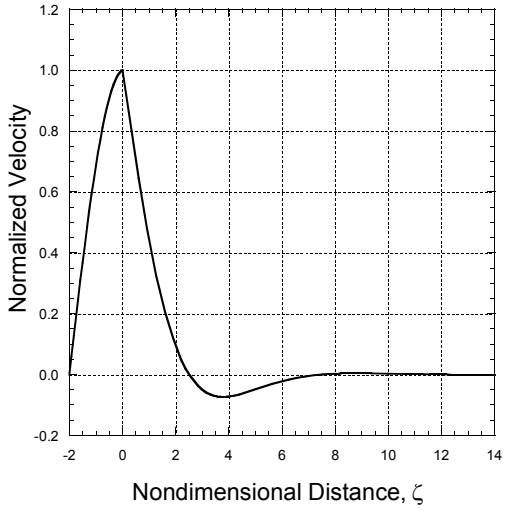

(a) R = 1

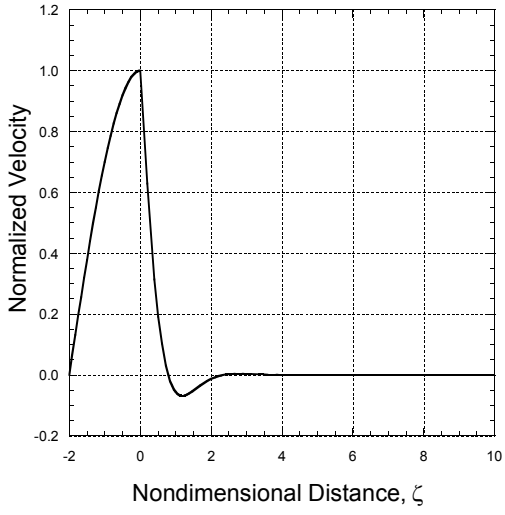

(b) R = 10

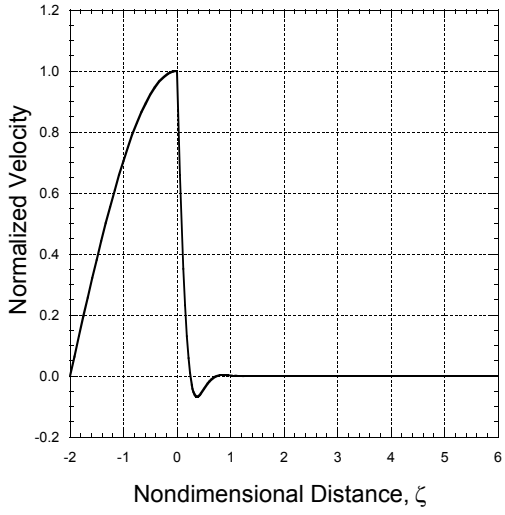

(c) R = 100

Fig. 3. Deformation field associated with the fundamental made depicted as a function of the nondimensional radial distance ς for various values of R when $\omega = \pi/4$ and ρ = 0.1.

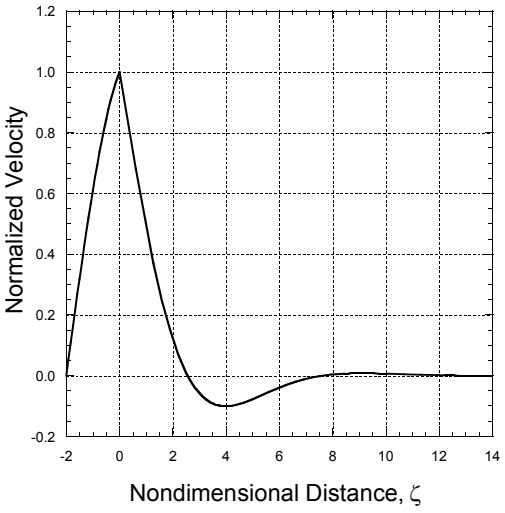

(a) $R = 1$

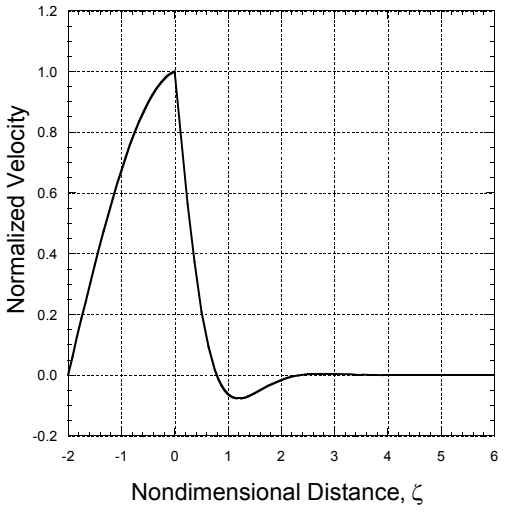

(b) $R = 10$

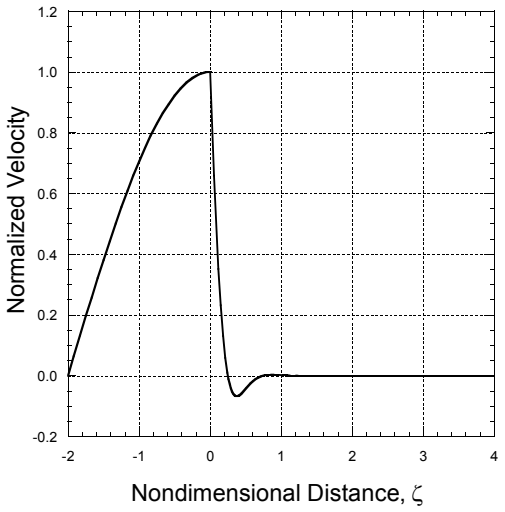

(c) $R = 100$

Fig. 4. Deformation field associated with the fundamental made depicted as a function of the nondimensional radial distance ς for various values of R when $\omega = \pi/4$ and $\rho = 0.5$.

For the fundamental torsional mode, instantaneous velocity field was calculated and displayed as a function of the axial distance ς from the fluid-solid interface. The velocity distribution in the fluid was obtained from Eq. (35) after substituting the expression B in Eq. (38). The velocity distribution in the solid was obtained from Eq. (32) after differentiating it with respect to time τ. Fig. 3 is the velocity profile for $\rho = 0.1$, and Fig. 4 is the velocity profile for $\rho = 0.5$. Figs. 3 and 4 display the velocity profile for (a) $R = 1$, (b) $R = 10$, and (c) $R = 100$. The plots were normalized by the velocity value at the solid-fluid interface at $\varsigma = 0$. The velocity field is shown for a relatively high-viscosity fluid, and thus the boundary layer in the fluid is relatively thick.

4. Approximate solutions

The exact solutions derived in Section 3 suffer from the disadvantage that ω and h are not expressed explicitly in terms of the parameters R and ρ. This disadvantage is resolved by employing the approximate approach instead of the exact solutions. In many applications R is fairly large. Thus it may be useful to obtain an asymptotic solution for large R. A new parameter ε is defined as $\varepsilon = R^{-1/2}$, and $\varepsilon << 1$ since $R >> 1$. Therefore, ε is considered as a perturbation and the approximate solution can be obtained by using the perturbation technique [9].

4.1 Perturbation series

The perturbation parameter ε is introduced to employ the stretched coordinate $\eta = \varsigma/\varepsilon$ for the fluid. Upon rescaling, the governing equations (21a) and (26) are transformed as follows:

$$\frac{d^2U}{d\varsigma^2} + [\, p^2 + (\omega + ih)^2]\, U = 0 \tag{42}$$

$$\frac{d^2V}{d\eta^2} - [\, -p^2\varepsilon^2 + i(\omega + ih)]\, V = 0 \tag{43}$$

Similarly, the boundary conditions (23a), (27), (17), and (18) are transformed as follows:

$$U(-l) = 0 \tag{44}$$

$$V(\infty) = 0 \tag{45}$$

$$V(0) = i(\omega + ih)\, U(0) \tag{46}$$

$$U'(0) = \rho\,\varepsilon^2 \cdot \frac{1}{\varepsilon}\frac{dV}{d\eta}\bigg|_{\eta=0} = \rho\,\varepsilon\, V'(0) \tag{47}$$

The case of $R \to \infty$ $(\varepsilon \to 0)$ corresponds to the classical torsional problem in a circular rod without an adjacent fluid or with an inviscid fluid.

For $R > 1$, i.e. $\varepsilon < 1$, the approximate solutions of the fundamental mode accept the following form:

$$U(\varsigma) = u_0(\varsigma) + \varepsilon\, u_1(\varsigma) + \varepsilon^2\, u_2(\varsigma) + \cdots \tag{48}$$

$$V(\eta) = v_0(\eta) + \varepsilon v_1(\eta) + \varepsilon^2 v_2(\eta) + \cdots \quad (49)$$

$$\omega = \omega_0 + \varepsilon \omega_1 + \varepsilon^2 \omega_2 + \cdots \quad (50)$$

$$h = \varepsilon h_1 + \varepsilon^2 h_2 + \cdots \quad (51)$$

The series of Eqs. (48)-(51) are substituted into Eqs. (42)-(47) and the coefficients of like powers in ε are equated. As a result, a sequence of boundary-value problems is obtained.

A solution developed in what follows, in the limit of $R \to \infty$, reduces to the fundamental mode ($p = 0$) of the classical case. Eqs. (42) and (43) are reduced to simpler forms as follows:

$$\frac{d^2U}{d\varsigma^2} + (\omega + ih)^2 U = 0 \quad (52)$$

$$\frac{d^2V}{d\eta^2} - i(\omega + ih)V = 0 \quad (53)$$

A similar procedure may be used for higher modes.

O (ε^0) in solid

For the leading order O (ε^0), the governing equation and boundary conditions in solid are as follows:

$$u_0'' + \omega_0^2 u_0 = 0 \quad (54)$$

$$u_0(-l) = 0 \quad (55)$$

$$u_0'(0) = 0 \quad (56)$$

Eqs. (54)-(56) are typical equations for torsional vibrations without the effect of an adjacent viscous fluid. The solution satisfying Eqs. (54)-(56) is as follows:

$$u_0(\varsigma) = U_0 \cos(\omega_0 \varsigma) \quad (57)$$

O (ε^0) in fluid

For the leading order O (ε^0), the governing equation and boundary conditions in fluid are as follows:

$$v_0'' + i\omega_0 v_0 = 0 \quad (58)$$

$$v_0(\infty) = 0 \quad (59)$$

$$v_0(0) = i\omega_0 u_0(0) \quad (60)$$

The solution satisfying Eqs. (58)- (60) is as follows:

$$v_0(\eta) = i\omega_0 U_0 \exp(-\sqrt{i\omega_0}\,\eta) = i\omega_0 U_0 \exp(-\frac{(1+i)\sqrt{\omega_0}}{\sqrt{2}}\eta) \quad (61)$$

O (ε^1) in solid

For the first order O (ε^1), the governing equation and boundary conditions in solid are as follows:

$$u_1'' + \omega_0^2 u_1 = -2\omega_0(\omega_1 + ih_1)u_0 \quad (62)$$

$$u_1(-l) = 0 \quad (63)$$

$$u_1'(0) = \rho v_0'(0) \quad (64)$$

Upon substituting u_0 and v_0 obtained earlier, the existence of the solution satisfying Eqs. (62)- (64) yields the following relations:

$$\omega_1 = -\frac{\rho}{\pi}\omega_0\sqrt{2\omega_0} = -\frac{\rho\sqrt{\omega_0}}{\sqrt{2}\,l} \quad (65)$$

$$h_1 = \frac{\rho}{\pi}\omega_0\sqrt{2\omega_0} = \frac{\rho\sqrt{\omega_0}}{\sqrt{2}\,l} \quad (66)$$

The solution is as follows:

$$\begin{aligned} u_1(\varsigma) &= -(\omega_1 + ih_1)U_0(\varsigma + l)\sin(\omega_0\varsigma) \\ &= -(i-1)\frac{\rho\sqrt{\omega_0}}{\sqrt{2}\,l}U_0(\varsigma + l)\sin(\omega_0\varsigma) \\ &= \frac{(1-i)}{\sqrt{2}}\rho\sqrt{\omega_0}\,U_0\left(\frac{\varsigma}{l}+1\right)\sin(\omega_0\varsigma) \end{aligned} \quad (67)$$

O (ε^1) in fluid

For the first order O (ε^1), the governing equation and boundary conditions in fluid are as follows:

$$v_1'' - i\omega_1 v_0 - i\omega_0 v_1 + h_1 v_0 = 0 \quad (68)$$

$$v_1(\infty) = 0 \quad (69)$$

$$v_1(0) = i\omega_0 u_1(0) + i(\omega_1 + ih_1)u_0(0) \quad (70)$$

The solution satisfying Eqs. (68)-(70) is as follows:

$$\begin{aligned} v_1(\eta) &= -\rho\frac{(1+i)\sqrt{\omega_0}}{\sqrt{2}\,l}U_0\exp(-\sqrt{i\omega_0}\,\eta) \\ &\quad + \frac{\rho}{2l}i\omega_0 U_0\,\eta\exp(-\sqrt{i\omega_0}\,\eta) \\ &= \left[-\frac{(1+i)\sqrt{\omega_0}}{\sqrt{2}} + \frac{i\omega_0}{2}\eta\right]\frac{\rho}{l}U_0\exp(-\sqrt{i\omega_0}\,\eta) \end{aligned} \quad (71)$$

O (ε^2) in solid

For the second order O (ε^2), the governing equation and boundary conditions in solid are as follows:

$$\begin{aligned} u_2'' + \omega_0^2 u_2 &= -2\omega_0(\omega_1 + ih_1)u_1 \\ &\quad -\left[2\omega_0(\omega_2 + ih_2) + (\omega_1 + ih_1)^2\right]u_0 \end{aligned} \quad (72)$$

$$u_2(-l) = 0 \quad (73)$$

$$u_2'(0) = \rho v_1'(0) \quad (74)$$

Upon substituting u_0, u_1, v_0, and v_1 obtained earlier, the existence of the solution satisfying Eqs. (72)-(74) yields the following relations:

$$\omega_2 = 0 \quad (75)$$

$$h_2 = -\frac{1}{2}\left(\frac{\rho\omega_0}{\pi}\right)^2 = -\frac{\rho^2}{2\,l^2} \tag{76}$$

The solution is as follows:

$$\begin{aligned} u_2(\varsigma) = & \left(\frac{\rho}{l}\right)^2 \frac{1}{4\omega_0} i U_0 \cos(\omega_0 \varsigma) + \frac{\rho^2}{l} i U_0 \sin(\omega_0 \varsigma) \\ & + \left[2\,\omega_0 \frac{\rho^2}{l} i U_0 \left(\frac{\varsigma}{l}+1\right)\left\{\frac{\varsigma}{2} - \frac{1}{4\omega_0}\sin(2\omega_0 \varsigma)\right\}\right. \\ & \left. - \frac{\omega_0}{2}\left(\frac{\rho}{l}\right)^2 i U_0 \varsigma^2 + \left(\frac{\rho}{l}\right)^2 \frac{1}{4\omega_0} i U_0 \cos(2\omega_0 \varsigma)\right] \cos(\omega_0 \varsigma) \\ & + \left[\frac{\rho^2}{2l} i U_0 \left(\frac{\varsigma}{l}+1\right)\cos(2\omega_0 \varsigma)\right. \\ & \left. + \left(\frac{\rho}{l}\right)^2 i U_0 \left\{\varsigma + \frac{1}{4\omega_0}\sin(2\omega_0 \varsigma)\right\}\right] \sin(\omega_0 \varsigma) \end{aligned} \tag{77}$$

4.2 Natural vibration characteristics

The sequence of boundary-value problems solved recursively provides the explicit expressions for u, v, ω, and h. Substituting Eqs. (57), (67), and (77) into Eq. (48) yields the displacement distribution of deformation in the solid rod. Similarly, substituting Eqs. (61) and (71) into Eq. (49) yields the velocity distribution of deformation in the viscous fluid.

Meanwhile, substituting Eqs. (65) and (75) into Eq. (50) yields the following form:

$$\omega = \omega_0 - \varepsilon \frac{\rho}{\pi} \omega_0 \sqrt{2\,\omega_0} + O(\varepsilon^3) \tag{78}$$

Similarly, substituting Eqs. (66) and (76) into Eq. (51) yields the following form:

$$h = \varepsilon \frac{\rho}{\pi} \omega_0 \sqrt{2\,\omega_0} - \varepsilon^2 \frac{1}{2}\left(\frac{\rho\,\omega_0}{\pi}\right)^2 + O(\varepsilon^3) \tag{79}$$

Eqs. (78) and (79) express approximately the natural frequency and damping rate of the torsionally-vibrating rod affected by the viscous fluid adjacent to the end face. Numerical results calculated with these equations for various cases of the fundamental mode are displayed in Fig. 2 with solid lines, and they are compared with the exact solutions. It is clear from Fig. 2 that for a wide range of R values, the approximate solution is in excellent agreement with the exact one. In the range of very small R, the approximate solution does not provide reasonable results, and the limitation of the approximate solution is identified.

As shown in Fig. 2, the natural frequency decreases and the damping rate increases as R decreases in the range of R values considered. This results from the fact that the thickness of the fluid boundary layer increases as R decreases.

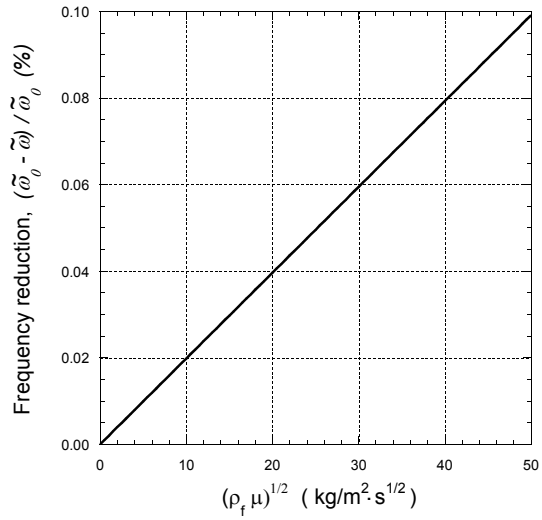

(a) Natural frequency, $\tilde{\omega}$

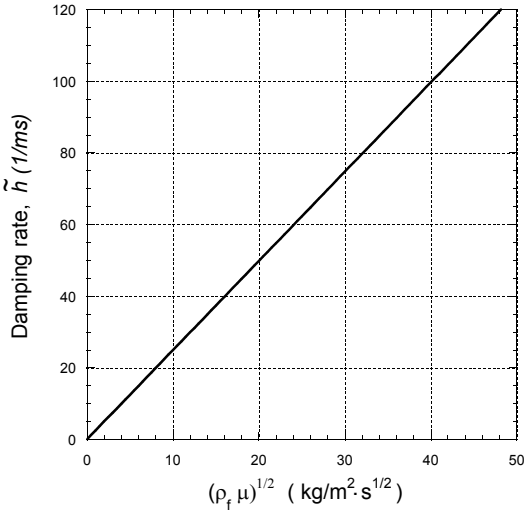

(b) Damping rate, $\tilde{h}$

Fig. 5. Dimensional natural frequency and damping rate depicted as a function of $(\rho_f\,\mu)^{1/2}$ for $\rho_s = 2.7\times10^3$ kg/m^3, $G = 24$ GPa, and $\tilde{\omega}_0 = 2\pi \times (20$ kHz).

To relate physically the natural frequency change and damping rate with the viscosity of the adjacent fluid, the terms up to the order of ε^1 are selected and physical dimensions are recovered as follows:

$$\frac{\tilde{\omega}_0 - \tilde{\omega}}{\tilde{\omega}_0} = \frac{1}{\pi}\sqrt{\frac{2\,\tilde{\omega}_0}{G\,\rho_s}}\sqrt{\rho_f\,\mu} \tag{80}$$

$$\tilde{h} = \frac{\tilde{\omega}_0}{\pi}\sqrt{\frac{2\,\tilde{\omega}_0}{G\,\rho_s}}\sqrt{\rho_f\,\mu} \tag{81}$$

Given with the material properties, such as the mass density and shear modulus, and the fundamental frequency in the absence of the viscosity effect, the natural frequency change and damping rate can be calculated and can show a relationship linearly-proportional to $(\rho_f\,\mu)^{1/2}$. For example, when $\rho_s =$

2.7×10^3 kg/m^3, G = 24 GPa, and $\tilde{\omega}_0 = 2\pi \times$ (20 kHz), the natural frequency change and damping rate are displayed as a function of $(\rho_f \mu)^{1/2}$ in Fig. 5. The range of $(\rho_f \mu)^{1/2}$ value in Fig. 5 is established to include a conventional viscous fluid such as glycerin at room temperature (ρ_f = 1,264 kg/m^3, μ = 1.492 kg/m·s).

The theoretical results in this paper are not compared with experimental ones. However, the previous research [10], which considered the effect of a viscous fluid at the circumferential face of a circular rod, compared the theoretical and experimental results and showed good agreement.

5. Conclusion

The effect of the viscosity of a fluid adjacent to the end face on the torsional vibration of a rod has been identified theoretically. The interaction problem has been formulated mathematically and then solved exactly and approximately for the vibration displacement of the rod and the vibration velocity of the fluid.

The approximate solution has been extended to express the natural frequency change and damping rate, which turn out to be proportional to the square root of the viscosity multiplied by mass density of the fluid. A comparison of the exact solution with the approximate one reveals that the latter is more useful for a wide range of application.

The result demonstrates that a rod vibrating torsionally at high frequency can be used as a sensor for measuring the viscosity of a fluid.

Acknowledgment

The authors acknowledge the contribution of Mr. Seung Mo Jung in calculating the approximate solutions.

Nomenclature

c_0 : Sound velocity in the rod
G : Shear modulus of the rod
h : Nondimensional damping rate
$\tilde{h}$: Damping rate
l : Ratio of length and radius of the rod
R : Variable of inversely proportional to the fluid viscosity
u : Nondimensional circumferential displacement of the rod
u_θ : Circumferential displacement of the rod
v : Nondimensional circumferential velocity of the fluid
v_θ : Circumferential velocity of the fluid
ε : Inverse of square root of R
η : Stretched coordinate of the fluid region
μ : The fluid viscosity
ρ : Mass density ratio of the fluid and the rod
ς : Nondimensional axial direction in cylindrical coordinates
τ : Nondimensional time
ω : Nondimensional natural frequency
$\tilde{\omega}$: Natural frequency
ξ : Nondimensional radial direction in cylindrical Coordinates

References

[1] J. O. Kim and H. Y. Chun, Interaction between the torsional vibration of a circular rod and an Adjacent viscous fluid, *ASME J. Vib. Acoust.*, 125 (2003) 39-45.
[2] R. F. Hafer and A. Laesecke, Extension of the torsional crystal viscometer to measurement in the time domain, *Meas. Sci. Technol.*, 14 (2003) 663-673.
[3] B. Jakoby, M. Scherer and H. Eisenschmid, An automotive engine oil viscosity sensor, *IEEE Sensors J.*, 3 (2003) 562-568.
[4] A. Agoston, C. Otsch and B. Jakoby, Viscosity sensors for engine oil condition monitoring, *Sensors and Actuators A*, 121 (2005) 327-332.
[5] J. O. Kim and O. S. Kwon, Vibration characteristics of the piezoelectric torsional transducers, *J. Sound Vib.*, 264 (2003) 453-473.
[6] J. D. Achenbach, *Wave Propagation in Elastic Solids*, *North-Holland Publ.*, Amsterdam (1975) p. 241, p.24.
[7] R. W. Fox and A. T. McDonald, *Introduction to Fluid Mechanics*, 5th ed., *John Wiley and Sons*, New York (1998) p. 709.
[8] S. Wolfram, *The Mathematica Book*, *Wolfram Media & Cambridge U. P.* (1999).
[9] A. H. Nayfeh, *Introduction to Perturbation Techniques*, *John Wiley & Sons*, New York (1981).
[10] H. Y. Chun and J. O. Kim, A Study on the measurement of the fluid viscosity by using the torsional vibration of a circular rod, *Transactions of KSME*, 26 (6) (2002) 1016-1025.

Jin Oh Kim was born in Seoul, Korea, in 1958. He received the B. S. and M. S. degrees in mechanical engineering from Seoul National University, in 1981 and 1983, respectively, and the Ph.D. degree from University of Pennsylvania, Philadelphia, in 1989. He worked at Korea Research Institute of Standards and Science, Northwestern University, and Samsung Advanced Institute of Technology. Since 1997, he has been with the Faculty of Soongsil University, where he is currently a Professor of mechanical engineering. His research interests are in the area of ultrasonic sensors and actuators using mechanical vibrations.